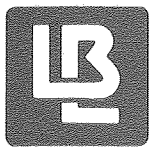

Lawrence Berkeley Laboratory
UNIVERSITY OF CALIFORNIA

ENERGY & ENVIRONMENT DIVISION

Submitted to Applied Physics

BREWSTER WINDOW AND WINDOWLESS RESONANT SPECTROPHONES FOR INTRACAVITY OPERATION

Robert Gerlach and Nabil M. Amer

April 1980

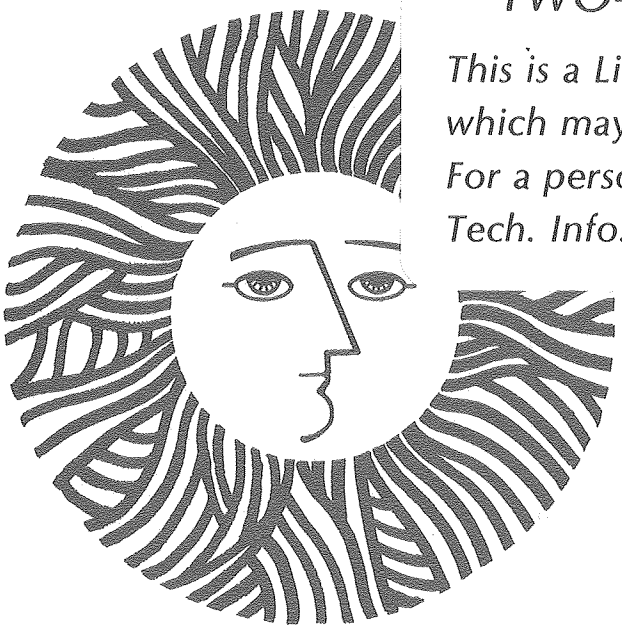

Prepared for the U.S. Department of Energy under Contract W-7405-ENG-48

DISCLAIMER

LBL-10877
Preprint

Lawrence Berkeley Laboratory
UNIVERSITY OF CALIFORNIA

ENERGY & ENVIRONMENT
DIVISION

Submitted to Applied Physics

BREWSTER WINDOW AND WINDOWLESS RESONANT SPECTROPHONES FOR INTRACAVITY OPERATION

Robert Gerlach and Nibil M. Amer

April 1980

Prepared for the U.S. Department of Energy under Contract W-7405-ENG-48

BREWSTER WINDOW AND WINDOWLESS RESONANT SPECTROPHONES FOR INTRACAVITY OPERATION

By

Robert Gerlach and Nabil M. Amer

Applied Physics and Laser Spectroscopy Group
Lawrence Berkeley Laboratory
University of California
Berkeley, California 94720
U. S. A.

PACS Codes 06, 07.65, 42.80

BREWSTER WINDOW AND WINDOWLESS RESONANT SPECTROPHONES FOR INTRACAVITY OPERATION

Abstract

We report a new design for an acoustically resonant spectrophone well suited for intracavity operation with widely tunable lasers. Operation with Brewster angle windows or in a windowless mode is possible, and high quality factors (560 and 509, respectively) are achieved. Windowless operation permits continuous monitoring of ambient air. We discuss factors limiting the sensitivity, $\sim 10^{-7}$ cm^{-1}, and present a double chopping scheme capable of significantly reducing the acoustical background encountered in windowless operation. The sensitivity of the spectrophone's performance to misalignment is also examined.

BREWSTER WINDOW AND WINDOWLESS RESONANT SPECTROPHONES FOR INTRACAVITY OPERATION

As acoustically resonant spectrophones began to be used in conjunction with lasers for trace gas analysis, it was quickly realized that their already high sensitivity to weak optical absorption could be further enhanced by use of a multipass geometry to increase the amount of absorbed power[1,2]. A comparable increase in absorbed power could be achieved by placing the spectrophone inside the cavity of a laser, where the increase is due to the higher intracavity beam power available for absorption.

A principal obstacle to intracavity operation is that for commonly used resonant spectrophone designs, in which the beam passes through the windows at normal incidence, the window reflection losses impair operation of the laser. A further problem is that if the beam enters and leaves the cell at points of high pressure amplitude, as is the case when the beam passes directly down the center of a cylindrical cell and a radial mode is excited, any window absorption can give rise to a spurious background signal due to window heating. This problem is not unique to intracavity spectrophones, but is particularly serious there because, when power becomes large enough to give a high signal to noise ratio, this coherent background signal becomes the main factor limiting sensitivity.

The insertion loss can be reduced by antireflection coating the windows, but single-layer A/R coatings are usable over only a limited range of wavelengths. It would be more advantageous to have the beam pass through the windows at Brewster's angle (θ_B), since for many commonly used optical materials such as fused silica and sodium chloride, θ_B is nearly constant over a wide range of wavelengths, and variations of θ_B with wavelength can

be tolerated since reflectivity increases very slowly for small deviations from θ_B. Thus, low reflectivity can be maintained over a wide range of wavelengths comparable or superior to that achievable with multilayer A/R coatings, facilitating intracavity operation with widely tunable lasers.

The problem of window heating can be alleviated by placing the windows at nodes of the mode being excited. Somewhere inside the cell, however, the beam must pass through a region where the mode has a high amplitude in order to excite it efficiently. The amplitude $A_j(\omega)$ of the j'th acoustical mode excited at frequency ω by absorption of light in the bulk of the gas is given by[3]

$$A_j(\omega) = F(\omega)\ (\alpha/V_c) \int p_j^*(\vec{r})\ I(\vec{r})\ dV \qquad (1)$$

where $f(\omega)$ is the resonance lineshape, α is the absorption coefficient, V_c is the cell volume, $I(\vec{r})$ is the laser intensity, and $p_j^*(\vec{r})$ is the j'th mode eigenfunction, normalized such that $\int p_j^* p_j dV = V_c$. The path of the beam through the spectrophone must be chosen so that the integral in (1) does not vanish. For most efficient excitation of the j'th mode, it is desirable that the integrand (and hence p_j^*) have the same sign throughout that rather small portion of the cell volume in which $I(\vec{r})$ differs significantly from zero.

For a spectrophone to be used for monitoring ambient air, it would be desirable to eliminate the windows altogether[4]. This would facilitate continuous sampling by induction of a slow flow of air through the cell. Absence of windows certainly solves the insertion loss and window heating problems, but it can greatly degrade the Q of the acoustical cavity

resonance. Again, the solution is to let the beam enter and leave the cell at pressure nodes, where holes in the walls will constitute a minimal perturbation.

Our spectrophone design[5], based on the above considerations, is shown in cross sectional top view in Figure 1. As for all cylindrical acoustical resonators, the pressure amplitude for the first radial mode is a maximum along the center axis of the cylinder, passes through zero at about 2/3 of the way out to the cylindrical wall, and reaches a negative extremum at the wall. The horizontally polarized beam enters through a window mounted virtually flush with the flat end wall, passes diagonally through the center of the cell, and exits through a window on the other flat wall. The entry and exit points are chosen to lie on a node of the first radial mode. In order for the beam to pass through the windows at Brewster's angle, the ratio of cell radius R to length L must be

$$R/L = (\alpha_{01} \tan \theta_B)/(2 \beta_{01}) = 0.7967 \, n \qquad (2)$$

where $\alpha_{01} = 1.2197$ is the first zero of $dJ_0(\pi\alpha)/d\alpha$, $\beta_{01} = 0.7655$ is the first zero of $J_0(\pi\beta)$, and n is the refractive index of the window material.

The 1-inch electret microphone is centered directly on the cell axis. This has two advantages. First, the flat microphone face mounts approximately flush with the flat end wall, and does not perturb the cell geometry as it would on the cylindrical wall. Second, the microphone is now at the absolute maximum of the first radial mode, where the pressure amplitude is 2.5 times larger than at the cylindrical wall, the usual microphone location. The latter advantage is partially offset by the fact that the

integral in (1), and hence the amplitude of the first radial mode, is now only about 2/3 as large as it would be for the same absorption coefficient if the beam were passing directly down the center axis of the cell.

A gas filling port was also located on the pressure node to avoid spoiling the cavity quality factor Q.

The same design is applicable to windowless operation; the beam simply enters through open holes instead of windows. However, there is no longer any requirement of horizontal polarization. Also, there is no longer a constraint on the ratio R/L, and it is therefore desirable for several reasons to make the ratio smaller. Smaller beam entrance holes can then be used without aperturing the beam, the importance of viscous losses on the flat end walls is reduced, and the first radial resonant frequency is moved farther from the relatively broad first longitudinal resonance, which is strongly excited by ambient room noise.

Our spectrophone was designed for use with NaCl Brewster windows, having refractive index 1.491 at wavelength 10 μm; thus (2) gives R/L = 1.188. (Our actual R/L was 1.190.) We also operated it without windows, even though, for reasons noted above, we expected that its R/L ratio was larger than optimal for windowless operation. We have investigated the performance of our spectrophone using a calibration mixture of 54 ppm of ethylene (C_2H_4) in nitrogen to determine responsivity or calibration, and using pure nitrogen to determine background signal levels. The light source for these experiments was a CO_2 laser tuned to the P(14) line in the 10.6 μm band, for which the absorption coefficient of ethylene has been measured by several authors[6-8], as summarized in Table I. Intensity modulation of the laser light was achieved by modulation of the laser

current. This was considerably quieter than using a mechanical chopper (although some sound was emitted from the laser plasma tube) and also facilitated intracavity operation of the spectrophone. At the first radial resonant frequency around 2.7 kHz a modulation depth of about 66% could be achieved; this rolled off to about 8% at 5 kHz.

The frequency response of the spectrophone could be studied by sweeping the frequency at which the laser current was modulated. The response obtained with windows on the cell appears in Figure 2. Only two resonances are observed in the 1-6 kHz range: the first radial resonance at 2.7 kHz and the much weaker second radial resonance at 5 kHz. The reason no other resonances are observed is that for other resonances, either the integral in (1) is zero due to symmetry considerations (mode amplitude zero throughout the cell) or else, although the mode is excited by the light, it has a node at the microphone (mode amplitude zero at the microphone only). The second radial mode is much more weakly excited than the first, partially because of the rolloff of the current modulator, as noted above, but also because the integrand in (1) is not of the same sign throughout the region where the beam is present, resulting in a partial cancellation. A high resolution scan of the first radial resonance yielded a value of 560 for the quality factor Q (defined here as the resonant frequency divided by the full width at $1/\sqrt{2}$ amplitude). We were able to do a similar frequency response study for windowless operation by allowing the 54 ppm ethylene mixture to flow in slowly through the gas fill port and out through the window holes. We found that removal of the windows only decreased the Q of the first radial resonance from 560 to 509.

Calibration of the spectrophone was performed with the spectrophone outside the laser cavity where the incident power could be determined more

accurately. The calibration consisted of determining the output voltage, and from this the sound pressure level, for a beam of known power passing through a gas sample of known absorption coefficient. The relevant data for calibration appear in Table II. A mixture of 54 ppm of ethylene in nitrogen gives a signal of 45 mV RMS per Watt of incident power. Using the average of the absorption coefficients listed in Table I, we know that the absorption coefficient for 54 ppm of C_2H_4 is $1.70 \times 10^{-3} cm^{-1}$, so we get an electrical signal of 26.5 volts per Watt cm^{-1} of absorbed power. This calibration depends on the microphone sensitivity, so it is more universal to express the calibration in terms of pressure amplitude. The microphone we used had a sensitivity of 11 mV/Pa and its output was amplified by a x10 preamplifier before measurement. Therefore, a 1 Volt rms output would correspond to a 9.1 Pa rms pressure amplitude. Our calibration in pressure units is 241 Pa/(W cm^{-1}). Finally, we must point out that the power we measured for this calibration was the average over many cycles of modulation, i.e., the d.c. component, and that in general this differs from the peak to peak amplitude of the fluctuating part of the power. For a different modulation depth, a different calibration factor could be expected. Purely by chance, it happened that at this frequency, the modulation depth of 66% was such that the peak to peak amplitude of the power modulation was approximately the same as the average power. Therefore, a comparable calibration factor could be expected for a mechanically chopped (i.e., modulation depth 100%) laser if the power used for normalization were, not as in our case the average power after modulation or chopping, but rather the power incident upon the mechanical chopper. The calibration will also depend somewhat on the modulation waveform, since only the fundamental Fourier component of that waveform

will be resonant with, and hence significantly excite, the first radial mode.

One of the pertinent questions we set out to answer in assessing the performance of our spectrophone was whether the chosen geometry did in fact minimize coherent background signal as intended, and how sensitive the background and calibration were to slight deviations of the beam path from that which was intended. Obviously, if the calibration varied significantly with small movements of the beam, then the accuracy of measurements made with the spectrophone would be adversely affected unless the spectrophone alignment were very carefully adjusted and rigidly fixed. A rapid increase in background due to beam devaition would likewise cause problems.

Our studies of the variation of calibration and background with beam path were done with NaCl Brewster windows on the spectrophone. In the data that follow we will express calibration, as above, in pressure amplitude in Pa per W cm^{-1} of absorbed power. We will express background signal both in terms of pressure amplitude per unit incident power (Pa/W) and also in terms of the equivalent bulk absorption coefficient (cm^{-1}) in the gas that would be necessary to produce the same pressure amplitude.

The variation of the background and calibration with horizontal translation of the beam perpendicular to its propagation direction is plotted in Figure 3a. As the beam moves, its interesection with one window moves away from a node toward a region of positive pressure amplitude, while the intersection with the other window moves toward a region of negative pressure amplitude. The window heating effects tend to cancel out to first order, and a rather broad minimum in background signal is observed. For large excursions the beam begins grazing the edges of the window aperture and the background signal increases rapidly.

For parallel translation of the beam, the angle of incidence upon the windows remains constant at θ_B, and there is no background contribution due to reflected beams heating the walls. These measurements were made with a beam focused to a diameter of less than 1 mm within the spectrophone in order to achieve good spatial resolution. If one were to use a beam having a spot size over which a significant variation of the background signal would occur, then the background signal one would observe would be a weighted average of the background plotted in Figure 3a over the area illuminated by the beam. We found that the cell calibration or response was very nearly invariant with horizontal movement of the beam. This is also expected to be constant to first order, but to decrease for sufficiently large excursions in either direction.

Another geometrical variable we investigated was the angular alignment of the beam in the horizontal plane, subject to the constraint that it must pass through the center point of the cell. This variation appears in Figure 3b. The angular deviation is positive when the angle of incidence on the windows (measured from the normal) is greater than θ_B. As the angle changes, one expects the contributions of window heating to have the same sign for both windows, so that for a given distance of movement of the beam on the window, a greater background signal would be produced than for an equivalent movement due to parallel translation of the beam. Also, as the angle of incidence deviates from θ_B, the window reflectivity becomes nonzero, and the reflected beam can heat the walls of the cell, making a further contribution to the background signal. These data also were taken with a focused beam, and whereas the focusing increased our spatial resolution for the data of Figure 3a, it decreased our angular resolution for the data of Figure 3b. Because the laser would only operate in a high

transverse mode, the focused beam had a large divergence of order 1 degree. Since these data already have a larger than normal angular spread folded in, it should usually not be necessary to make any further allowances for angular beam spread in extracting a sensitivity or background signal level. The data of Figure 3b show that a rather asymmetric minimum in background does occur for the intended beam path, and that it is safer to have the angle of incidence slightly too large rather than too small. The response was expected to fall off monotonically with increasing angle, but actually levels off and rises again slightly for the largest angles examined. This is a preferable behavior since the derivative of response with respect to beam angle is closer to zero in the vicinity of Brewster's angle, but the physical explanation for this behavior is presently unknown to us.

We have also looked at vertical translation of the beam position perpendicular to its propagation direction. As with the horizontal position data, the response depends very weakly on vertical position of the beam. The background also displays a rather broad flat minimum, since as the beam moves vertically, its intercepts with the windows move tangentially to the nodal circles and never depart very far from the nodes.

A final variable we investigated was the polarization angle of the beam. The response is independent of the polarization provided that one corrects for the reflection loss at the windows. However, the background signal depends strongly on polarization angle, as shown in Figure 4. The beam path is fixed, and all the increase in background signal observed is attributable to the increase in heating of the walls by the beam reflected from the exit window. The polarization angle is measured with respect to the plane of incidence, 0° being pure horizontal polarization. When the angle of incidence is θ_B, the reflectivity R_p for polarization in the

plane of incidence is zero, so the reflectivity for a beam polarized at angle ψ with respect to the horizontal plane is given by $R_s \sin^2 \psi$, where R_s is the reflectivity for polarization perpendicular to the plane of incidence, about 0.144 for NaCl. For small departures from horizontal polarization this sine-squared dependence appears parabolic, as exhibited by the data of Figure 4. The data indicate that a deviation of several degrees from horizontal polarization can be tolerated. Since we know how reflectivity varies with polarization, we can determine how much reflected power is causing the observed background signal, and we find that one milliwatt of reflected power gives a background pressure amplitude of 3.2×10^{-5} Pa, equivalent to an absorption of 1.3×10^{-7} W cm^{-1} in the gas.

In the summary, we have found that the calibration and background signal are not terribly sensitive to slight misalignments of the beam. The most serious difficulties are caused by tilting of the beam in the horizontal plane such that the angle at which it passes through the spectrophone changes, and greatest care should be taken in performing this alignment.

Now we proceed to the more crucial question of what are the factors limiting the sensitivity that can be achieved with this type of spectrophone. We classify these in three categories:

1) Noise, by which we mean any random fluctuation, electronic or acoustical, which does not bear a fixed phase relation with the modulation of the laser intensity.
2) Coherent acoustical background, by which we mean signal caused by the modulation process, but not attributable to the presence of the light beam in the spectrophone. In our case this is due to sound emitted by the current-modulated laser. This signal is at the same

frequency as, and locked in phase with respect to, the laser intensity modulation.

3) Coherent photoacoustic background. This is a signal caused by the laser beam, but not due to absorption of light in the bulk of the gas. Rather it is due to heating of windows by the beam and heating of the spectrophone walls by reflected or scattered light. It, too, is at the same frequency and locked in phase with the laser intensity modulation.

Noise has a broadband frequency spectrum, and can be reduced by narrowband filtering of the signal, as is done in phase sensitive detection. The two types of coherent background, however, are extremely narrowband signals at the same frequency as the modulation, and hence cannot be eliminated by filtering. The coherent photoacoustic background has the further problem that, since it is proportional to the laser power, no improvement can be achieved by increasing the power, since signal and background increase in proportion to one another.

The magnitudes of these limiting factors for the case of operation with Brewster windows are listed in Table III. We have expressed each of these in several different sets of units: voltage, pressure amplitude, equivalent absorption coefficient that would give the same pressure amplitude, and the concentration of ethylene that would be required to give that much absorption. In certain cases it is necessary to multiply or divide by the laser power P and/or the square root of the bandwidth B in order to determine the actual levels that would be observed in practice. The random noise level of 1 $\mu V/Hz^{1/2}$, for example, must be multiplied by $B^{1/2}$. This noise level is about 10 times the expected electronic noise level for our preamplifier at this frequency and source impedance,

and is believed to be predominantly acoustical noise. No acoustical shielding of the spectrophone was used. To get the noise-equivalent absorption one must multiply 3.8×10^{-8} W cm^{-1} $Hz^{-1/2}$ by $B^{1/2}P^{-1}$. In order to get an idea of the sensitivity that can be achieved for a representative trace gas, the equivalent ethylene concentration that would give the same signal level is also tabulated. To get the noise-equivalent ethylene concentration, multiply 1.2×10^{-9} W $Hz^{-1/2}$ by $B^{1/2}P^{-1}$. For the case of intracavity operation, the intracavity power was so high that this noise was equivalent to an ethylene concentration of 25×10^{-12}, or 25 parts per trillion, with a 1 Hz detection bandwidth. However, as we shall see, noise was not the principal limiting factor for our sensitivity.

Our coherent acoustical background was 20 μV or 1.8×10^{-4} Pa, equivalent to an absorption of 7.5×10^{-7} W cm^{-1}. To get the equivalent absorption coefficient divide this latter number by P. This background signal is dependent on the location of the spectrophone in relation to sound sources associated with the modulation process.

The coherent photoacoustic background, whose dependence on geometrical variables we have discussed earlier, was 5.5 μV/W, or 5×10^{-5} Pa/W, assuming the beam was optimally aligned. This is equivalent to an absorption coefficient of 2.1×10^{-7} cm^{-1} or an ethylene concentration of 6.6 parts per billion, independent of the laser power. Since the noise and coherent acoustical background can be made negligible by using high power, as is done in intracavity operation, this coherent photoacoustic background will be the ultimate limit on sensitivity.

The magnitudes of sensitivity limiting factors for windowless operation appear in Table IV. When the spectrophone was operated without windows, ambient room noise was much more significant. First, there were several

low frequency noise sources which, while well outside our detection band, impaired operation by overloading the electronics. There was a Helmholtz resonance of the cavity at 300 Hz which was strongly excited by ambient room noise, and typically gave signals on the order of 10 mV. And there were pressure transients caused by the change in room pressure when a door was opened or closed. Some degree of immunity to these low-frequency noise sources was gained by use of a 1 kHz high-pass filter. Much more of a problem was the first longitudinal resonance at 2.66 kHz. While the spectrophone was designed to retain a high Q for the first radial mode even when the windows were removed, this design did not give a high Q for longitudinal modes because the holes were located at pressure maxima for those modes. The first longitudinal resonance was very broad, and was strongly excited by ambient noise, resulting in a large noise contribution at the frequency of the first radial resonance. As mentioned earlier, if the spectrophone were intended solely for windowless operation, this problem could be alleviated by making the radius to length ratio smaller, reducing the proximity of the two modes. It is interesting that it was relatively difficult to excite the first radial mode with ambient room noise. We tried exciting the cell with sound from a loudspeaker and found that the radial resonance was always hard to detect on the tail of the longitudinal resonance. Noise levels for windowless operation were around 5 $\mu V/Hz^{1/2}$, or 4.5×10^{-5} $Pa/Hz^{1/2}$, for a quiet day in the lab and no flow of gas through the spectrophone. Assuming the cell calibration remained roughly the same as when windows were present, this would be equivalent to an absorption of about 2×10^{-7} W cm^{-1} $Hz^{-1/2}$. Inducing a flow of gas into the cell made things much worse.

The coherent acoustical background was 114 μV, or 1 x 10^{-3} Pa, equivalent to an absorption of about 4.4 x 10^{-6} W cm^{-1}.

In the absence of windows, one would not expect any coherent photoacoustic background (except perhaps for heating of the walls by light scattered from aerosols). Verification of this expectation was made difficult by the high levels of noise and coherent acoustical background, and also by the ambiguity caused by actual bulk absorption by the air in the cell due to water vapor, etc. The absorption could be eliminated by continuously flushing the cell with nitrogen, but this exaggerated the noise problem, so static laboratory air was used.

In order to solve the problem of high coherent acoustical background we adopted a double-chopping scheme. (The method to be described is useful whenever the sensitivity is limited by coherent acoustical background, as from a loud chopper, but does nothing to alleviate random noise that could not be accomplished equally well with a single stage of phase sensitive detection with the same net system bandwidth.) The laser was current-modulated at the spectrophone's resonant frequency of 2.7 kHz; its output was then passed through a 1 Hz mechanical chopper. The microphone signal was fed to a first lock-in amplifier referenced to the 2.7 kHz laser modulation, with a time constant of 12.5 msec (10 Hz bandwith). The output of this first lock-in was then fed to a second lock-in referenced to the 1 Hz chopper and having a 3 sec time constant (0.04 Hz net system bandwidth). The use of the chopper made it possible to isolate that component of the 2.7 kHz microphone signal which was specifically due to the presence of the laser beam passing through the cell. The low chopping frequency was necessary in order to allow adequate time for the high Q cavity ringing to decay when the beam was blocked and build up again when the beam was present.

Using the above method, we measured a coherent photoacoustic signal of 7.6 μV/W for the P(14) line. This is slightly greater than the coherent photoacoustic background observed with windows on the cell, but in this case, since there is air rather than nitrogen in the cell, the signal may be attributable to absorption by water vapor or other constituents of the atmosphere. In order to determine whether water vapor could account for the signal, we compared the signal obtained for the P(14) line to that obtained for the R(20) line at 10.247 μm, which is very strongly absorbed by water vapor[9]. For the R(20) line we measured 54 μV/W, so the ratio of P(14) signal to R(20) signal was 0.14. The ratio of water vapor absorption coefficients for these two lines ranges from 0.07 to 0.14 as the partial pressure of water vapor ranges from 5 to 15 torr[9]. The photoacoustic signal for R(20) indicates an absorption coefficient of about 2×10^{-6} cm^{-1}, which would require a water vapor concentration of less than 5 torr[9]. Therefore, it appears that the observed P(14) signal is somewhat too large to be accounted for entirely by water vapor absorption and that roughly half, or 4 μV/W, was due to either coherent photoacoustic background or absorption by other gases or aerosols in the air. This is equivalent to a pressure amplitude of 3.6×10^{-5} Pa/W, or an absorption coefficient of 1.5×10^{-7} cm^{-1}.

One possible disadvantage of our spectrophone in windowless operation is that the ratio of hole surface area to total cell volume is rather small, so that as the composition of ambient air changes, it takes a relatively long time for such changes to appear in the spectrophone by diffusion, and a more active circulation method may be necessary. In this respect the design presented by Shtrikman and Slatkine[4] may be preferable. However, our design could be improved by drilling a number

of small holes ($\sim$ 6 mm dia.) along the intersections of the nodal cylinder with the end plates so as to give better circulation while preserving a high Q for the first radial mode.

In conclusion, we have presented a design for a resonant spectrophone which is well suited to operation inside a laser cavity due to its low optical insertion losses. The insensitivity of these losses to wavelength makes it suitable for use with widely tunable lasers such as dye lasers. The high intracavity powers obtainable with lasers such as CO_2, together with the low coherent background, make possible the detection of very weak absorption. The spectrophone can be operated with windows, for analysis of samples of gas introduced through a fill port, or can be operated without windows, with reduced sensitivity, for monitoring ambient air. We envisage applications for such a spectrophone in pollution detection and in detection of absorption due to very weak transitiitions, such as high overtone bands in molecules.

This work was supported by the U. S. Department of Energy under Contract No. W-7405-ENG-48.

REFERENCES

1. C. F. Dewey, R. D. Kamm, and C. E. Hackett, Appl. Phys. Lett. 23, 633-635 (1973).
2. E. Max and L.-G. Rosengren, Opt. Commun. 11, 422-426 (1974).
3. L. B. Kreuzer, "The Physics of Signal Generation and Detection," in Y.-H. Pao, ed., Optoacoustic Spectroscopy and Detection (Academic Press, New York, 1977), pp. 1-25.
4. Another design for a windowless resonant spectrophone, differing drastically from ours, was presented by S. Shtrikman and M. Slatkine, Appl. Phys. Lett. 31, 830-831 (1977).
5. A preliminary report on this design was presented at the O.S.A. Topical Meeting on Photoacoustic Spectroscopy, Ames, Iowa, Aug. 1-3, 1979.
6. R. R. Patty, G. M. Russwurm, W. A. McClenny, and D. R. Morgan, Appl. Opt. 13, 2850-2854 (1974).
7. W. Schnell and G. Fischer, Appl. Opt. 14, 2058-2059 (1975).
8. A. Mayer, J. Comera, H. Charpentier, and C. Jaussaud, Appl. Opt. 17, 391-393 (1978).
9. M. S. Shumate, R. T. Menzies, J. S. Margolis, and L.-G. Rosengren, Appl. Opt. 15, 2480-2488 (1976).

Figure Captions

1. Cross sectional top view of the spectrophone
2. Frequency response of the spectrophone from 1 KHz to 6 KHz measured with windows attached.

3a. Variation of the spectrophone calibration and coherent photoacoustic background signal with horizontal translation of the beam.

3b. Variation of the spectrophone calibration and background signal with horizontal tilting of the beam.

4. Variation of the coherent photoacoustic background signal with deviation of the beam polarization angle from the horizontal.

Table Captions

Table I. Measurements of the Absorption Coefficient of C_2H_4 at the CO_2 00°1-10°0 P(14) Line at 10.529 μm.

Table II. Cell Calibration

Table III. Factors limiting sensitivity when the spectrophone is operated with windows.

Table IV. Factors limiting sensitivity in windowless operation.

Table I.

Reference	Measured Absorption Coefficient ($atm^{-1}cm^{-1}$)
Patty *et al.* [6]	29.10[a]
Schnell & Fisher [7]	33.0 [b]
Mayer *et al.* [8]	32.14[a]
Average	31.4

[a]Measures at 760 Torr total pressure

[b]Measured at 360 Torr total pressure

Table II.

Signal for 5.4×10^{-5} atm of C_2H_4	$4.5 \times 10^{-2} \frac{V}{W}$
Absorption Coefficient of C_2H_4 (Average from Table I)	$31.4\ atm^{-1}cm^{-1}$
Signal per Unit Power per Unit Absorption Coefficient	$26.5 \frac{V}{W\ cm^{-1}}$
Microphone Sensitivity	$1.1 \times 10^{-2} \frac{V}{Pa}$
Preamplifier Gain	10
Pressure Amplitude per Unit Absorption Coefficient per Unit Power	$241 \frac{Pa}{W\ cm^{-1}}$

Table III.

	RMS	Equivalent RMS Pressure	Equivalent Absorption	Equivalent C_2H_4 Concentration
Noise	$1 \frac{\mu V}{Hz^{1/2}}$	$9 \times 10^{-6} \frac{Pa}{Hz^{1/2}}$	$3.8 \times 10^{-8} \frac{W\ cm^{-1}}{Hz^{1/2}}$	$1.2 \times 10^{-9} \frac{W}{Hz^{1/2}}$
Coherent Acoustical Background	20 μV	1.8×10^{-4} Pa	7.5×10^{-7} W cm^{-1}	2.4×10^{-8} W
Coherent Photoacoustic Background	5.5 μV/W	$5 \times 10^{-5} \frac{Pa}{W}$	2.1×10^{-7} cm^{-1}	6.6×10^{-9}

Table IV.

	RMS Voltage	Equivalent RMS Pressure	Equivalent Absorption[a]	Equivalent C_2H_4 Concentration[a]
Noise	$\geq 5 \frac{\mu V}{Hz^{1/2}}$	$\geq 4.5 \times 10^{-5} \frac{Pa}{Hz^{1/2}}$	$\geq 1.9 \cdot 10^{-7} \frac{W\ cm^{-1}}{Hz^{1/2}}$	$\geq 6.0 \times 10^{-9} \frac{W}{Hz^{1/2}}$
Coherent Acoustical Background	114 μV	1.0×10^{-3} Pa	4.3×10^{-6} W cm^{-1}	1.4×10^{-7} W
Coherent Photoacoustic Background	$\leq 4 \frac{\mu V}{W}$	$\leq 3.6 \times 10^{-5} \frac{Pa}{W}$	$\leq 1.5 \times 10^{-7}$ cm^{-1}	$\leq 4.8 \times 10^{-9}$

[a] It is assumed in these columns that the calibration is unchanged by removal of the windows.

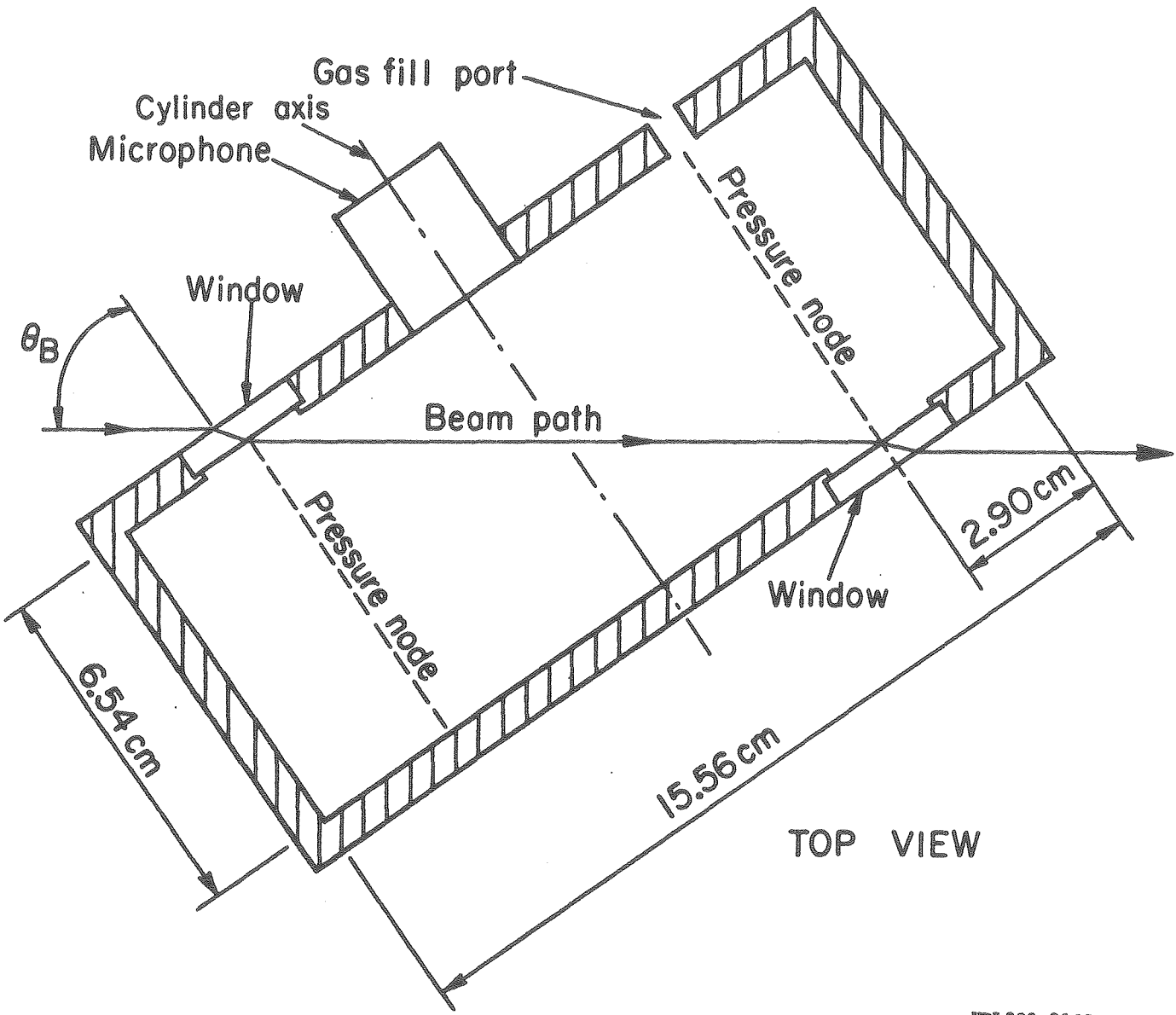
Gas fill port
Cylinder axis
Microphone
Window
θ_B
Beam path
Pressure node
Pressure node
Window
2.90cm
6.54cm
15.56cm
TOP VIEW
XBL803-3125

Figure 1.

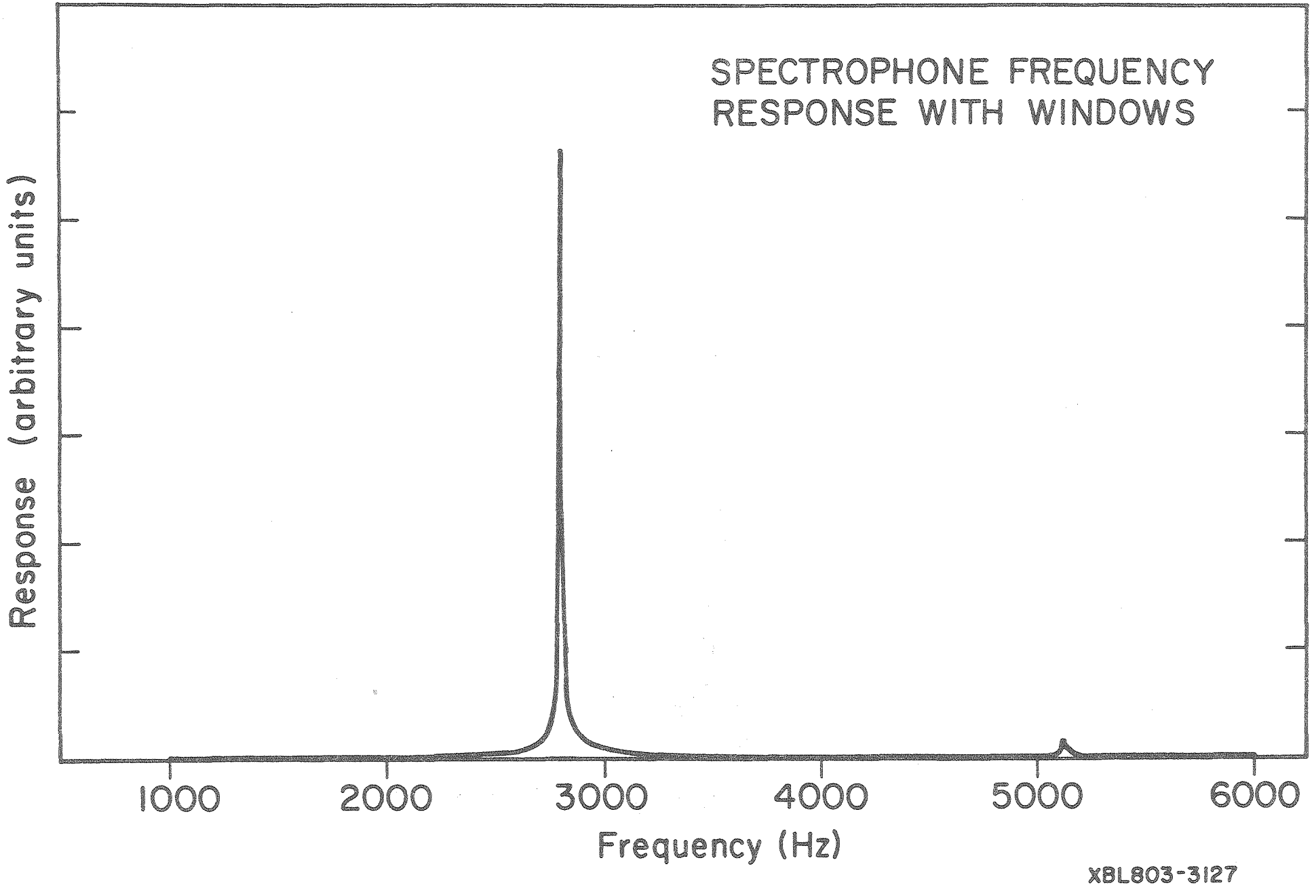
SPECTROPHONE FREQUENCY
RESPONSE WITH WINDOWS
Response (arbitrary units)
1000
2000
3000
4000
5000
6000
Frequency (Hz)
XBL803-3127

Figure 2.

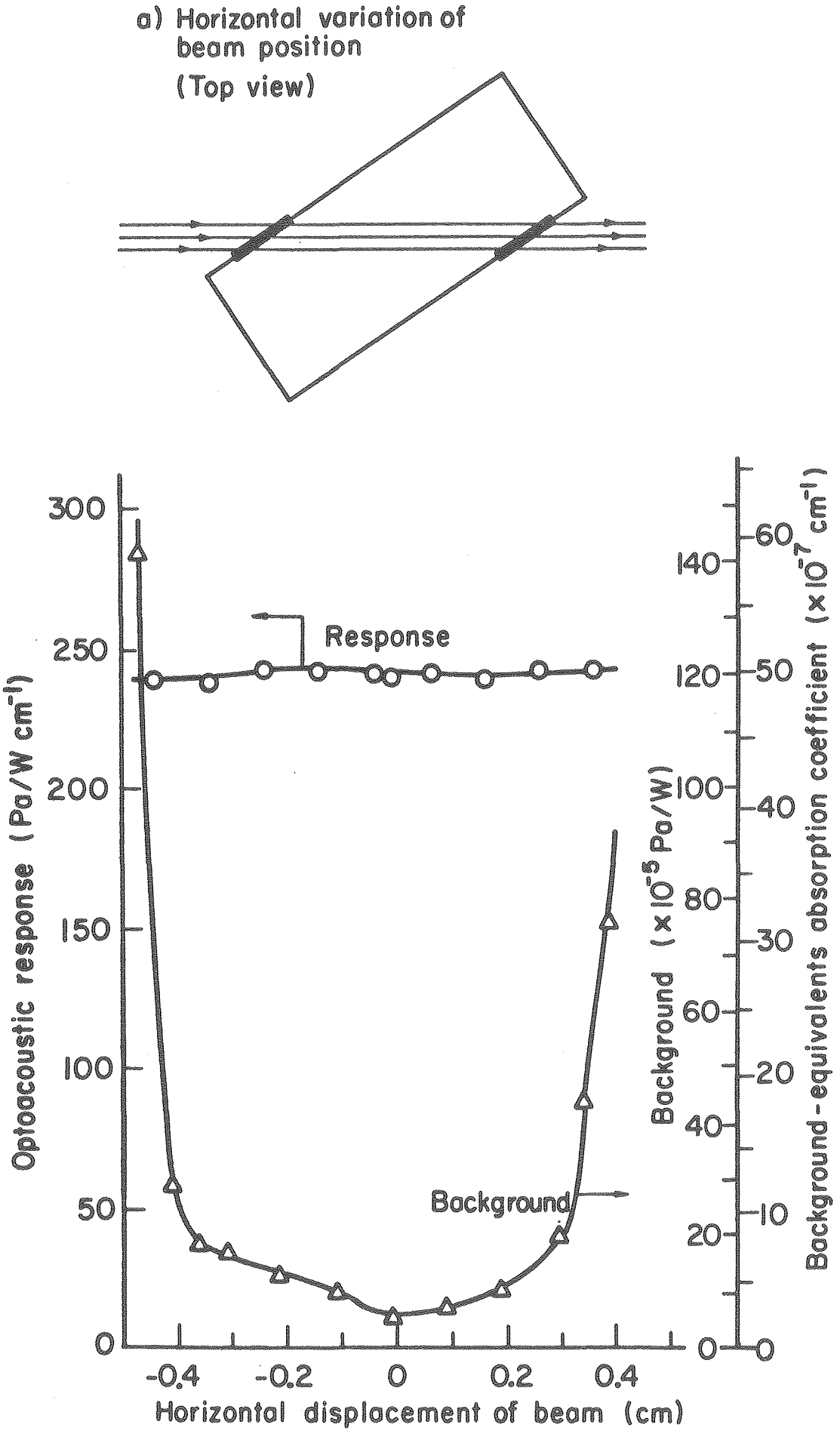

Figure 3a.

XBL 803-3130

b) Variation of beam angle
(Top view)

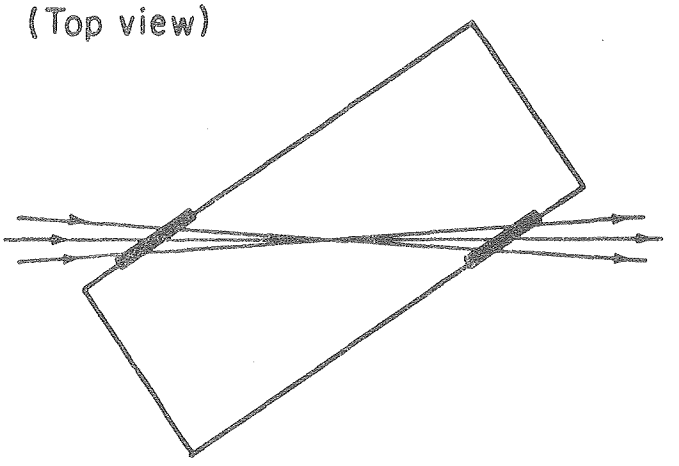

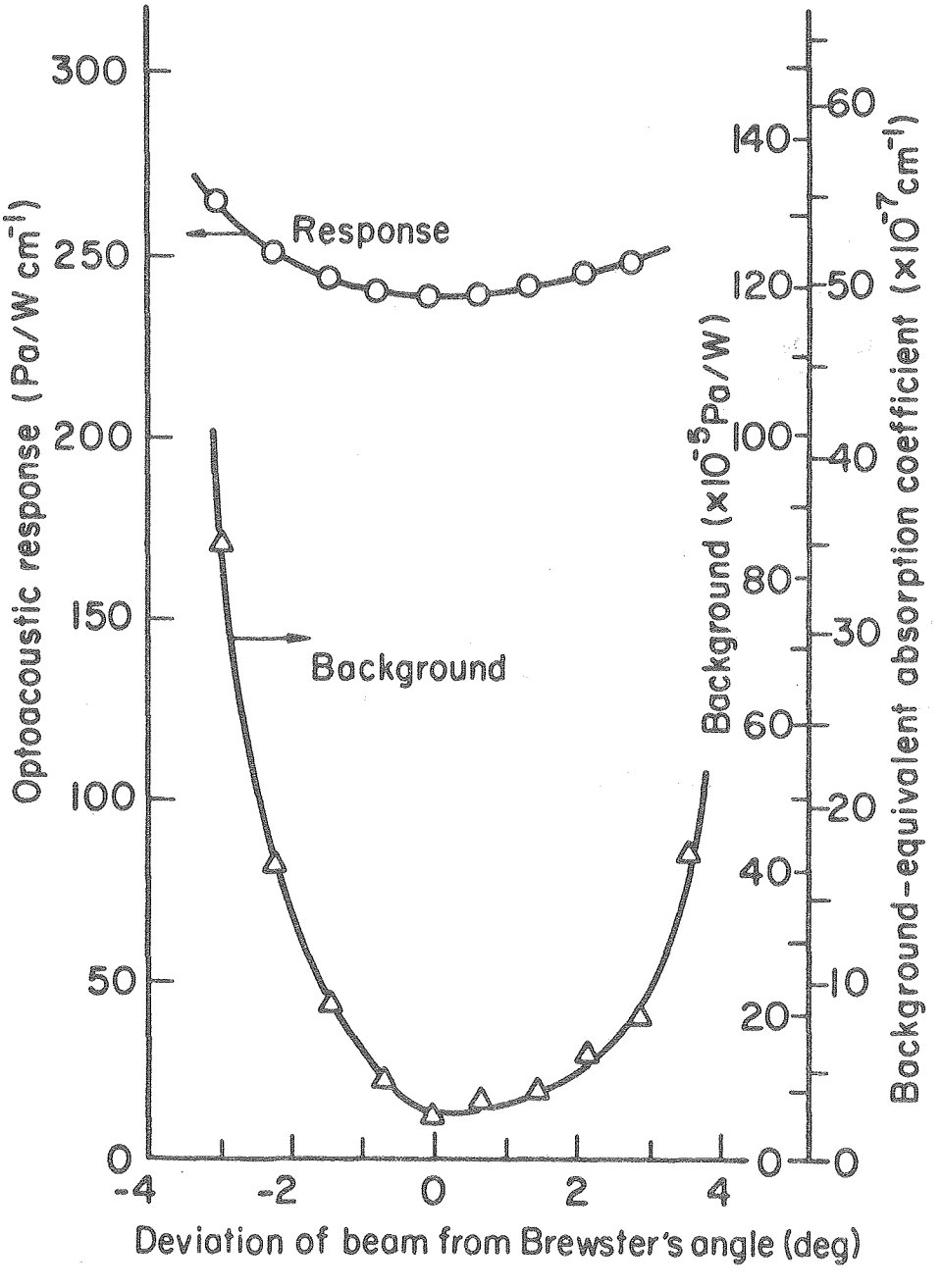

Figure 3b.

XBL803-3131

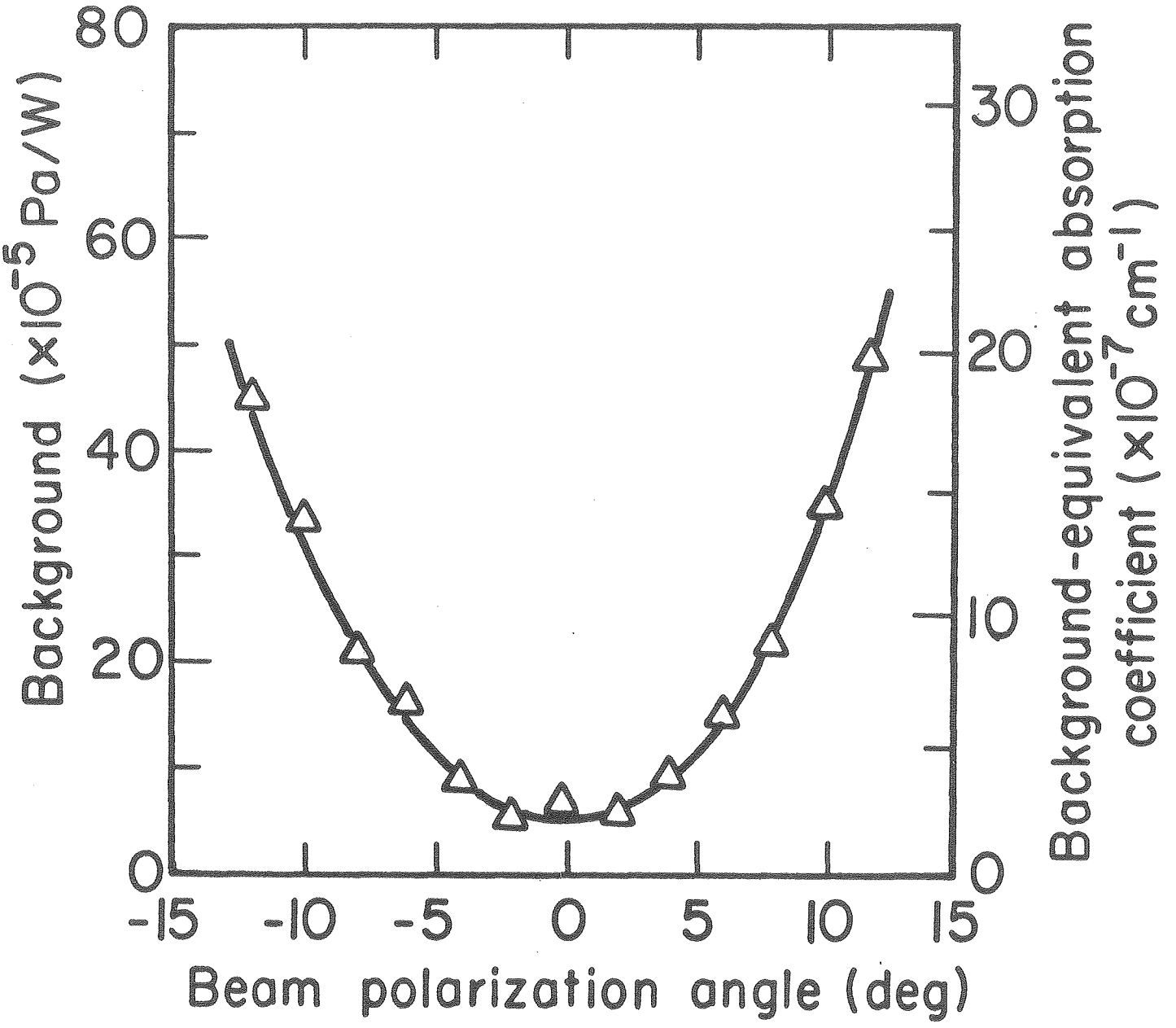

Figure 4.

XBL803-3126

TECHNICAL INFORMATION DEPARTMENT
LAWRENCE BERKELEY LABORATORY
UNIVERSITY OF CALIFORNIA
BERKELEY, CALIFORNIA 94720